Intrafollicular location of marginal zone/CD1d^hi B cells is associated with autoimmune pathology in a mouse model of lupus

Biyan Duan[1,*], Haitao Niu[1], Zhiwei Xu[1], Arlene H Sharpe[2], Byron P Croker[1,3], Eric S Sobel[4] and Laurence Morel[1]

Marginal zone (MZ) B cells contain a large number of autoreactive clones and the expansion of this compartment has been associated with autoimmunity. MZ B cells also efficiently transport blood-borne antigen to the follicles where they activate T cells and differentiate into plasma cells. Using the B6.NZM2410.*Sle1.Sle2.Sle3* (B6.TC) model of lupus, we show that the IgM$^+$ CD1d^{hi}/MZ B-cell compartment is expanded, and a large number of them reside inside the follicles. Contrary to the peripheral B-cell subset distribution and their activation status, the intrafollicular location of B6.TC IgM$^+$ CD1d^{hi}/MZ B cells depends on both bone marrow- and stromal-derived factors. Among the factors responsible for this intrafollicular location, we have identified an increased response to CXCL13 by B6.TC MZ B cells and a decreased expression of VCAM-1 on stromal cells in the B6.TC MZ. However, the reduced number of MZ macrophages observed in B6.TC MZs was independent of the IgM$^+$ CD1d^{hi}/B-cell location. B7-2 but not B7-1 deficiency restored IgM$^+$ CD1d^{hi}/MZ B-cell follicular exclusion in B6.TC mice, and it correlated with tolerance to dsDNA and a significant reduction of autoimmune pathology. These results suggest that follicular exclusion of IgM$^+$ CD1d^{hi}/MZ B cells is an important B-cell tolerance mechanism, and that B7-2 signaling is involved in breaching this tolerance checkpoint.

The marginal zone (MZ) is an anatomically distinctive region surrounding the follicles in the spleen, and it is composed mostly of B cells, specialized macrophages (marginal zone macrophages, MZMs), and stromal cells, but very few T cells.[1] The location of MZ B cells puts them on the first line of defense against blood-borne pathogens, and they possess unique properties to accomplish this function.[2] MZ B cells are long lived and noncirculating, and they respond to a wide spectrum of T-dependent (TD) and T-independent (TI) antigens by migrating into the follicle, where they can activate naive T cells more efficiently than follicular B cells and quickly differentiate to plasma cells.[3,4]

The location of MZ B cells results from the integration of many factors. Circulating B cells express high levels of CXCR5 that direct them to the follicular B-cell area, where CXCL13 is highly expressed.[5] In spite of their CXCR5 expression, MZ B cells are retained in the MZ through their surface expression of LFA-1 and $\alpha4/\beta1$ binding to ICAM-1 and VCAM-1, both expressed at high levels by the MZ stromal cells.[6] MZ B cells also express high levels of the sphingosine 1-phosphate (S1P) receptors S1P$_1$ and S1P$_3$ that are quickly downregulated upon antigen encounter, releasing MZ B cells toward the follicles.[7,8] MZMs also retain B cells in the MZ through contact by the scavenger receptor MARCO.[9] Conversely, MZ B cells are also necessary for the retention and maintenance of MZMs.[10]

The MZ B-cell compartment, which is enriched with autoreactive specificities,[11–13] is expanded in the (NZB × NZW)F$_1$ (BWF1) murine model of lupus,[14] and this expansion has been implicated in lupus pathogenesis.[15–17] Moreover, the massive enlargement of the MZ B-cell compartment resulting from BAFF overexpression is associated

[1]Department of Pathology, Immunology and Laboratory Medicine, University of Florida College of Medicine, Gainesville, FL, USA; [2]Harvard Medical School, Boston, MA, USA; [3]Pathology and Laboratory Medicine Service, Malcolm Randall VAMC, Gainesville, FL, USA and [4]Department of Medicine, Division of Rheumatology and Clinical Medicine, University of Florida, Gainesville, FL, USA

Correspondence: Dr L Morel, PhD, Department of Pathology, Immunology and Laboratory Medicine, University of Florida College of Medicine, JHMHSC M-632, 1600 SW Archer Road, Gainesville, FL 32610-0275, USA.
E-mail: morel@ufl.edu
  *Current address: Pathology Department, UT Southwestern Medical Center, Dallas, TX 75390-9072, USA.

with a lupus-like phenotype.[18] We have recently characterized a BWF1-derived NZM strain, TAN, which does not produce anti-dsDNA IgG antibodies (Abs) and is protected from lupus nephritis in spite of the presence of the three NZM2410-*Sle* lupus susceptibility loci.[19] Interestingly, TAN mice present an enlarged nonfunctional MZ B-cell compartment that expresses high level of CD5,[19] a marker that has been associated with tolerance in anergic B cells,[20] indicating a correlation between tolerization of MZ B cells and disease protection. Also in the NZM model, high affinity anti-DNA Ab producing B cells co-expressing the *Sle2* locus and the transgenic 56R immunoglobulin heavy chain that break tolerance to nuclear antigens are heavily skewed toward the MZ compartment.[21] Sequestration of autoreactive B cells into the MZ area has been proposed as a mechanism to prevent autoimmunity,[16] with this process being inefficient in lupus-prone MRL.lpr mice.[22]

The goal of this study was to examine the MZ B-cell compartment in the NZM2410-derived B6.NZM2410-*Sle1. Sle2.Sle3* (B6.TC) lupus model.[23] We have previously shown that the MZ is greatly reduced to absent in both NZM2410 and B6.TC, and that it contains very little B cells, although the percentage of cells that express MZ B surface markers is higher in these two strains than in the nonautoimmune control strain C57BL/6 (B6).[19] We have now explored these apparently contradictory observations in the B6.TC strain, which presents the advantage of developing fully penetrant lupus nephritis with only about 6% of the NZM2410 genome, and therefore allows the use of H-2^b-matched B6 as a valid experimental control. We found that the B6.TC MZ not only lacks B cells but also MZMs, and that the B6.TC B cells that express CD1d^hi, a surface marker expressed on the great majority of B6.TC MZ B, are largely located inside the follicles. This CD1d^hi B-cell population presents the same characteristics as that of normal MZ B cells after LPS exposure.[24] The intrafollicular location of the B6.TC CD1d^hi/MZ B cells could be explained at least partially by their enhanced migration to CXCL13 and S1P, whereas the MZ area expressed lower levels of VCAM-1. We also showed that the intrafollicular location of B6.TC CD1d^hi/MZ B cells depends on both bone marrow (BM) and stromal factors. In addition, we found that B7-2, but not B7-1 deficiency, restored a normal to increased CD1d^hi B-cell population in the B6.TC MZ area as well as a dramatic reduction in autoimmune pathology. This latter result strongly suggests that B7-2 signaling is involved in the intrafollicular location of CD1d^hi/MZ B cells and it is involved in autoimmune pathology.

MATERIALS AND METHODS
Mice
The production of the triple congenic B6.TC (listed in the JAX® mice database as BcN/LmoJ) and CD80 (B7-1) or CD86 (B7-2)-deficient B6 mice has been previously described.[23,25] For the production of B6.TC.B7-1^−/− and

B6.TC.B7-2^−/−, homozygosity at the *Sle1*, *Sle2*, and *Sle3* loci as well as the B7-1 and B7-2 null alleles was detected by PCR as previously described.[23,25] B6 and C57BL/6J-*Cg-Igha-Thy1aGpila/J* (B6.IgH^a) mice were obtained from the Jackson Laboratories and bred at the University of Florida. All experiments were conducted according to protocols approved by the University of Florida Institutional Animal Care and Use Committee. Both male and female mice were used in approximately equal numbers with sex- and age-matched B6 controls at 6- to 9-month old, or at 2–3 months when indicated.

Flow Cytometry
Splenocytes were stained with fluorochrome- or biotin-conjugated monoclonal Abs against B220 (RA3-6B2), CD1d (3C11), CD4 (RM4-5), CD5 (53-7.3), CD11a (2D7), CD19 (1D3), CD23 (B3B4), CD29 (Ha2/5), CD69 (H1.2F3), CD80 (16-10A), CD86 (GL1), IgD (217-170), IgM (II/41), IgM^a (Igh6a), IgM^b (B682), CD93 (AA4.1), and TNP (G235-2356), from BD Pharmingen or eBioscience, depending on the fluorochrome. Anti-MD-1/RP105 (MD14) was obtained from eBioscience and anti-BAFF-R (204406) from R&D Systems. The 7E9 clone, which binds equally to the CD21 (CR2) NZW and B6 alleles, was a gift from Dr Susan Boackle (University of Colorado, Denver, CO). Biotinylated Abs were detected with streptavidin-PerCP-Cy5.5 (BD Pharmingen) or streptavidin-APC-Cy7 (eBioscience). Samples were analyzed with either a BD FACSCalibur flow cytometer (Becton Dickinson) or Cyan (Dako), and at least 80 000 cells were acquired per sample.

Immunofluorescence Staining
Cold acetone-fixed 7 µm frozen spleen sections, first blocked with 10% rat serum, were stained with fluorochrome- or biotin-conjugated Abs: anti-mouse metallophilic macrophage (MOMA-1; Serotec), SIGN-R1 (ER-TR9; BMA Biomedicals), B220 (RA3-6B2), CD1d (1B1), CD5 (53-7.3), IgM (II/41), ICAM (3E2), VCAM-1 (429) and anti-TNP (G235-2356) (all from BD Pharmingen), and CD21 (7E9). Biotinylated Abs were detected with streptavidin-Alexia 568 (Molecular Probes). Sections were then mounted with Prolong Gold Mounting Media (Molecular Probes) and analyzed with a Zeiss Axiom fluorescent microscope.

Bone Marrow Chimeras
Reciprocal BM chimeras between B6.TC and B6.IgH^a were performed as previously described.[26] Briefly, Septra (sulfamethoxazole and trimethoprim; Hi-Tech Pharmaceutical)-treated 2-month-old recipient mice were irradiated twice with 525 rad 1 × 10^7 T cell-depleted BM cells from 4 to 6 week old mice were tail-vein injected in each irradiated mouse. Recipient mice were maintained for 3–8 months, as indicated, before analysis.

Migration Assay

For each sample, 1×10^6 splenocytes were first equilibrated in culture medium (10 mM HEPES, 10% FCS, $1 \times$ Pen/Strep in RPMI 1640) in the upper chamber of $5 \mu m$ of microporous transwell plates (Corning) for 1 h at 37°C. Then 100 ng/ml recombinant mouse CXCL13 (R&D Systems) or 1 nM S1P (Cayman Chemical) was added to the lower chamber. Flow cytometry analysis was conducted on cells migrated to the lower chamber after 2 h as well as on the original input cells to calculate the migration ratio.

In Vivo and In Vitro MZ B-Cell Ficoll Binding Assay

For in vivo assays, mice were killed 30 min after i.p. injection with $30 \mu g$ TNP-Ficoll (Biosearch). Anti-TNP Ab revealed Ficoll uptake on spleen frozen sections. For in vitro assays, splenocytes were incubated with TNP-Ficoll for 30 min at 37°C. Flow cytometry analysis was then conducted on thoroughly washed cells. For the LPS mobilization assay, mice were killed 3 h after i.p. injection with $10 \mu g$ LPS and CD1d^{hi} B-cell location was determined by immunofluorescence on splenic frozen sections.

Antibody Measurements

Anti-dsDNA and chromatin IgG auto-Abs, total IgM, and IgG levels were detected by ELISA assays as previously described.[23] Relative units of anti-dsDNA and anti-chromatin IgG were standardized using an NZM2410 serum, setting the reactivity of a 1:100 dilution of this control serum to 100 units.

Splenic and Renal Histology

The evaluation of glomerular lesions used a classification based on modifications of the WHO and RPS/ISN Classification of Glomerulonephritis in Systemic Lupus Erythematosus with a semiquantitative overlay on a 0–4 scale, as previously detailed.[27] Immune complexes in the kidneys were visualized on $8 \mu M$ frozen sections stained with FITC-conjugated anti-C3 (Cappel) and anti-IgG γ chain

(Jackson Immunoresearch). Staining intensity was evaluated in a blind fashion on a semiquantitative 0–3 scale and averaged on at least 10 glomeruli per section. Detection of glomerular macrophages was performed by averaging the number of CD68$^+$ (Serotec) cells in 10 randomly selected high-power fields.[27] MZ thickness was evaluated on hematoxylin and eosin (H&E) spleen sections comparatively to B6. MZ thickness in B6 mice is 5 ± 1 cell layers (mean and standard deviation, $N = 10$). MZ 'reduced' was scored as when MZs averaged three cell layers or less on at least 10 follicles, and MZ 'hyperplasia' when this average was seven cell layers or more. Mice were scored as MZ 'normal' when their MZ averaged 4–6 cell layers.

Statistical Analysis

Data were analyzed with the GraphPad Prism 4 software. Parametric or nonparametric were used as indicated, depending on whether the data was normally distributed. For multiple comparisons, ANOVA was used and selected pair comparisons were computed using the appropriate correction. Correlations were evaluated with the F statistic testing the null hypothesis that the linear regression slope was equal to 0. Distributions between two groups were compared using χ^2-tests. Statistical significance was obtained when $P \leq 0.05$.

RESULTS

CD1d^{hi}/MZ B Cells are Absent from the B6.TC MZ and Present in the Follicles

B6.TC mice showed a decrease of CD23 expression on IgM$^+$ B cells in 2-month-old mice that were accentuated with age (Table 1). The percentage of CD23$^+$ B cells was inversely correlated with anti-dsDNA IgG production ($P < 0.05$) and CD4$^+$ T-cell activation as measured by CD69 expression ($P < 0.002$) in B6.TC mice (Supplementary Figure 1). This suggests that the loss of CD23 + B cells is associated with the expression of lupus disease markers. The three B-cell subsets that express low levels of CD23 (plasma cells, transitional T1, and MZ B cells) are all expanded in B6.TC mice.[19,27,28] MZ B

Table 1 Comparison between B6.TC and B6 mice of the percentages of IgM$^+$ B cells expressing CD23, and the number of MZ B cells gated either as IgM$^+$ B220$^+$ CD21$^+$ CD23$^-$ or B220$^+$ CD21$^+$ CD1d^{hi}

	N per strain	B6.TC	B6	P
IgM$^+$ ($\times 10^6$) (2 months)	6	9.72 ± 3.10	4.85 ± 0.43	0.027
(6–8 months)	16	67.45 ± 8.80	19.52 ± 2.35	<0.0001
CD23$^+$ % of IgM$^+$ (2 months)	6	45.92 ± 3.66	57.65 ± 2.42	0.018
CD23$^+$ % of IgM$^+$ (6–8 months)	16	26.44 ± 2.58	73.89 ± 2.08	0.0001
IgM$^+$ B220$^+$ CD21$^+$ CD23$^-$ (10^6)	6	12.41 ± 0.43	2.75 ± 0.02	0.001
B220$^+$ CD21$^+$ CD1d^{hi} (10^6)	6	6.16 ± 0.32	1.68 ± 0.01	0.01

Means and standard errors, and P-values of t-tests.

cells, gated either as IgM^{+} B220^{+} CD21^{+} CD23^{−} or B220^{+} CD21^{+} CD1d^{hi}, were found in significantly greater percentages (Figures 1a and b) and numbers (Table 1) in B6.TC than in B6 spleens. B220^{+} CD1d^{hi} cells are overly represented in MZ B cells,[29,30] and about 50% of them are CD21^{+} CD23^{−} in our B6 mice (Figure 1c). Interestingly, this proportion was significantly higher in B6.TC mice, reaching over 80% (Figure 1c). These B cells did not express AA4.1 and CD5 (Figure 1d), and therefore displayed all the classical surface markers that have been described on MZ B cells.

In spite of the increased size of the MZ B compartment, B6.TC IgM^{+} or IgM^{+} CD1d^{hi} cells were absent or greatly reduced in the MZ area outside the MOMA-1^{+} layer that lines the marginal sinus (Figure 2a). The majority of these cells, however, were located inside the B6.TC follicles, which were comparatively devoid of follicular B cells (Figure 2b). Given (1) the expanded MZ B population characterized by surface markers, (2) the absence of B cells in the MZ area, and (3) the presence of numerous IgM^{+} CD1d^{hi} cells inside the follicle, over 80% of which are MZ B cells, we conclude that the majority of B6.TC MZ B cells are located inside the follicles. MZ macrophages were only found in small discontinuous MZ portions and scattered outside the MZ area

in B6.TC mice (Figure 2c), which was consistent with the reciprocal requirement of MZMs and MZ B cells for their maintenance in the MZ.[9,10]

### Both BM-Derived and Stromal Cells Contribute to B6.TC IgM^{+} CD1d^{hi} Cell Intrafollicular Location

Reciprocal BM chimeras between B6.IgH[a] and B6.TC mice were performed to dissect the mechanism responsible for the intrafollicular location of IgM^{+} CD1d^{hi} B cells in B6.TC mice. Overall decreased CD23 expression was observed only on B cells from B6.TC origin (data not shown), resulting in an enlarged transitional T1 compartment (Figure 3a), and reduced follicular B-cell subset (data not shown). However, the size of the MZ B compartment was significantly reduced in B cells of B6.TC origin (either transferred into B6.TC or B6 recipients), which contrasted with unmanipulated mice in which the percentage of B6.TC MZ B cells was increased (Figures 1 and 3b). The same results were obtained at either 3 months (Figure 3) or 8 months (data not shown) post-transfer. Flow cytometry performed on IgM[a] and IgM[b]-gated populations confirmed that all B cells originated from the transferred BM of B6.IgH[a] or B6.TC origin, respectively. Contrary to unmanipulated mice, IgM^{+} CD1d^{+} MZ B cells were prominently located on both sides of the marginal sinus
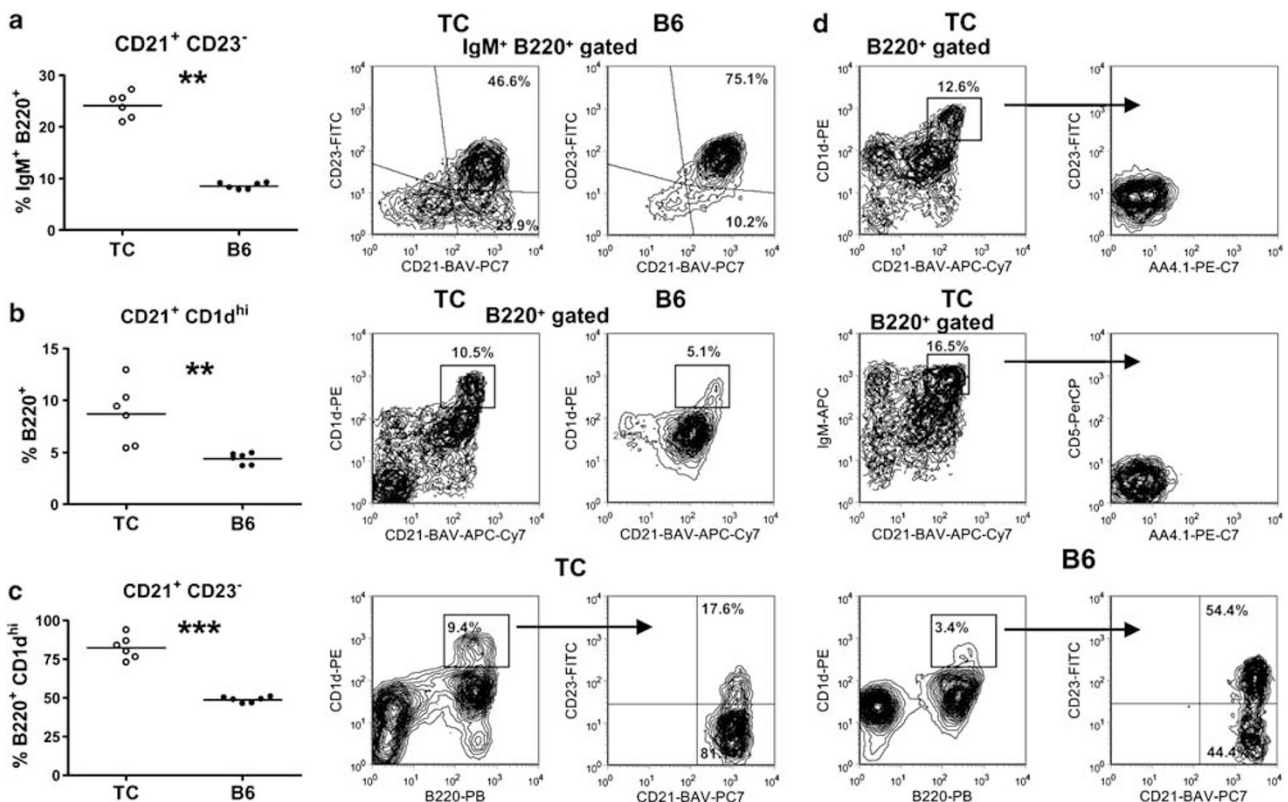
Figure 1 B6.TC mice produce significantly more MZ B cells identified either as IgM^{+} B220^{+} CD21^{+} CD23^{−} (**a**) or B220^{+} CD21^{+} CD1d^{hi} (**b**). (**c**) The B220^{+} CD1d^{hi} subset contains a significantly greater percentage of CD21^{+} CD23^{−} MZ B cells in B6.TC than in B6 mice. Representative FACS plots with their respective gates are shown on the right. (**d**) B6.TC B220^{+} CD21^{+} CD1d^{hi} cells are CD23^{−} AA4.1^{−} (top) and B220^{+} CD21^{+} IgM^{hi} are AA4.1^{−} and CD5^{−} (bottom), establishing that B6.TC MZ B cells have a normal B220^{+} CD21^{+} CD23^{−} CD1d^{hi} AA4.1^{−} CD5^{−} surface marker phenotype. **P < 0.01, ***P < 0.001.

in both B6.TC→B6.IgH^a and B6.IgH^a→B6.TC chimeras 3 months after transfer (Figure 3c). Control B6→B6 and B6.TC→B6.TC syngeneic chimeras showed an IgM$^+$ CD1d^{hi} cell distribution similar to that of the corresponding unmanipulated mice (Figure 3c), indicating that the results obtained with the reciprocal chimeras were not biased by the B-cell homeostatic expansion in the irradiated recipients.

Our results indicate that B6 stromal factors were sufficient to maintain some B6.TC IgM$^+$ CD1d^{hi}/MZ B cells in the MZ area, but that B6.TC stromal factors could not drive all the B6 IgM$^+$ CD1d^{hi}/MZ B cells inside the follicle. On the other hand, a substantial amount of IgM$^+$ CD1d^{hi}/MZ B cells were located inside the follicles in both types of chimeras, and the overall results suggest that both BM- and stromal-derived
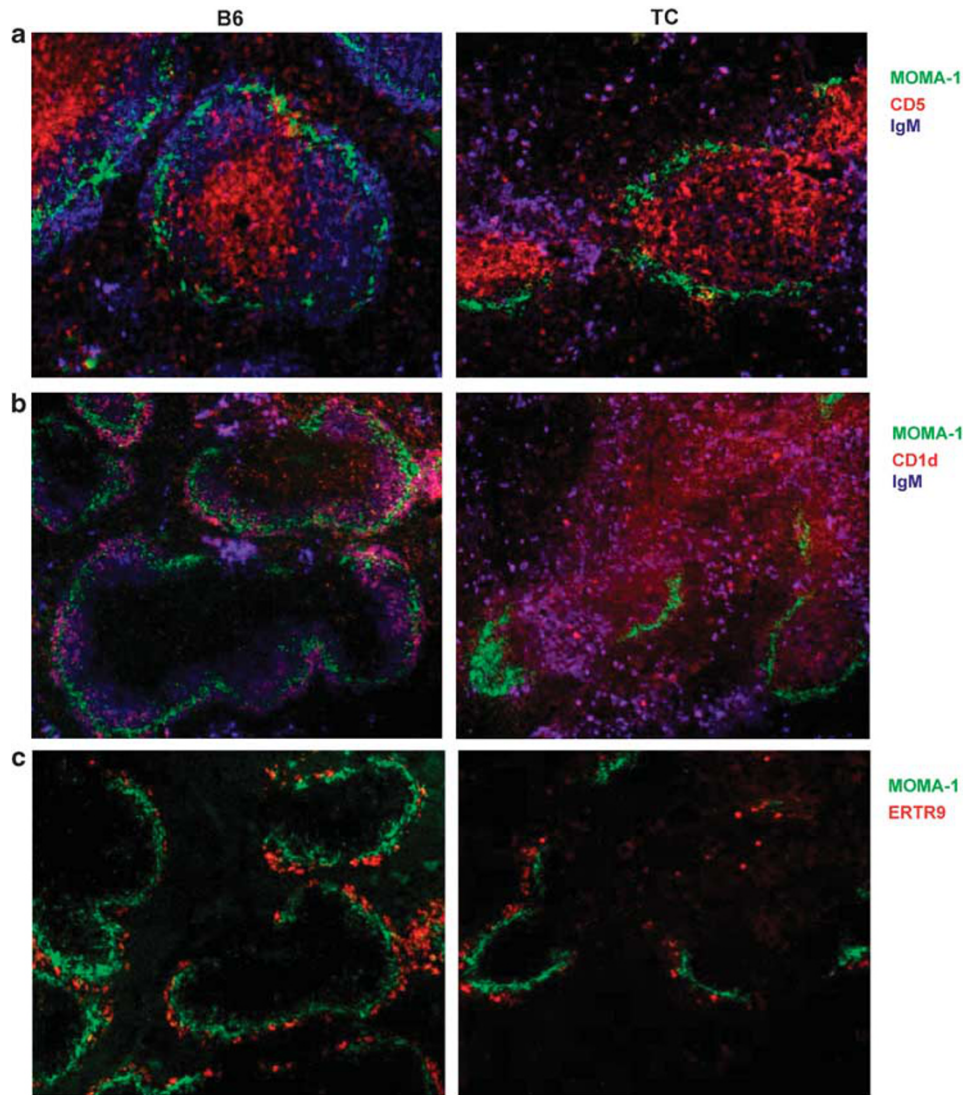

Figure 2 Representative spleen sections of >20 B6 (left) and B6.TC (right) 7- to 8-month-old mice showing MZ B cells as IgM^{hi} (**a**) or IgM^{hi} CD1d^{hi} (**b**) relative to the MOMA-1$^+$ metallophilic macrophages, and SIGNR-1$^+$ (ETR-9) MZMs (**c**). Panel a also shows T cells as CD5^{hi}, and panels a and b show a large number of IgM$^+$ plasma cells in the red pulp of B6.TC mice (magnification ×100).

Figure 3 Hematopoietic cell contribution to B-cell subset distribution and follicular location. Distribution of B220$^+$ CD21^{lo} CD23$^-$ T1 (**a**) and B220$^+$ CD21^{hi} CD23$^-$ MZ B cells (**b**) in irradiated B6.TC mice transferred with B6.IgH^a BM (heavy hatched bars), irradiated B6.IgH^a mice transferred with B6.TC BM (light hatched bars), as well as the syngeneic control chimera (gray bars) 3 months after transfer. Black and white bars represent age-matched unmanipulated B6.IgH^a and B6.TC respectively. Means and s.e. of five mice per group. t-Tests were performed between BM chimeras and between unmanipulated mice, ***P<0.001. (**c**) Representative spleen sections from B6.IgH^a BM→B6.TC mice (top left) and B6.TC BM→B6.IgH^a mice (top right) showing IgM$^+$ CD1d$^+$ cells on both sides of the MOMA-1$^+$ ring in both groups. Control B6.IgH^a BM→B6 (bottom left) and B6.TC BM→B6.TC (bottom right) chimeras showed IgM$^+$ CD1d$^+$ cell distribution similar to that of unmanipulated mice. (**d**) Normal number and distribution of SIGNR-1$^+$ MZMs in B6.IgH^a BM→B6.TC mice but not in B6.TC BM→B6.IgH^a mice (magnification ×100).

factors contribute to B6.TC MZ B-cell intrafollicular location. Histological examination of spleens 8 month post-transfer was not informative, as most of the follicular

structures disappeared in both types of chimeras, as it is commonly the case in older B6.TC and NZM2410 mice.[19,31] This suggested that similar to the IgM^{+} CD1d^{hi}/MZ B-cell
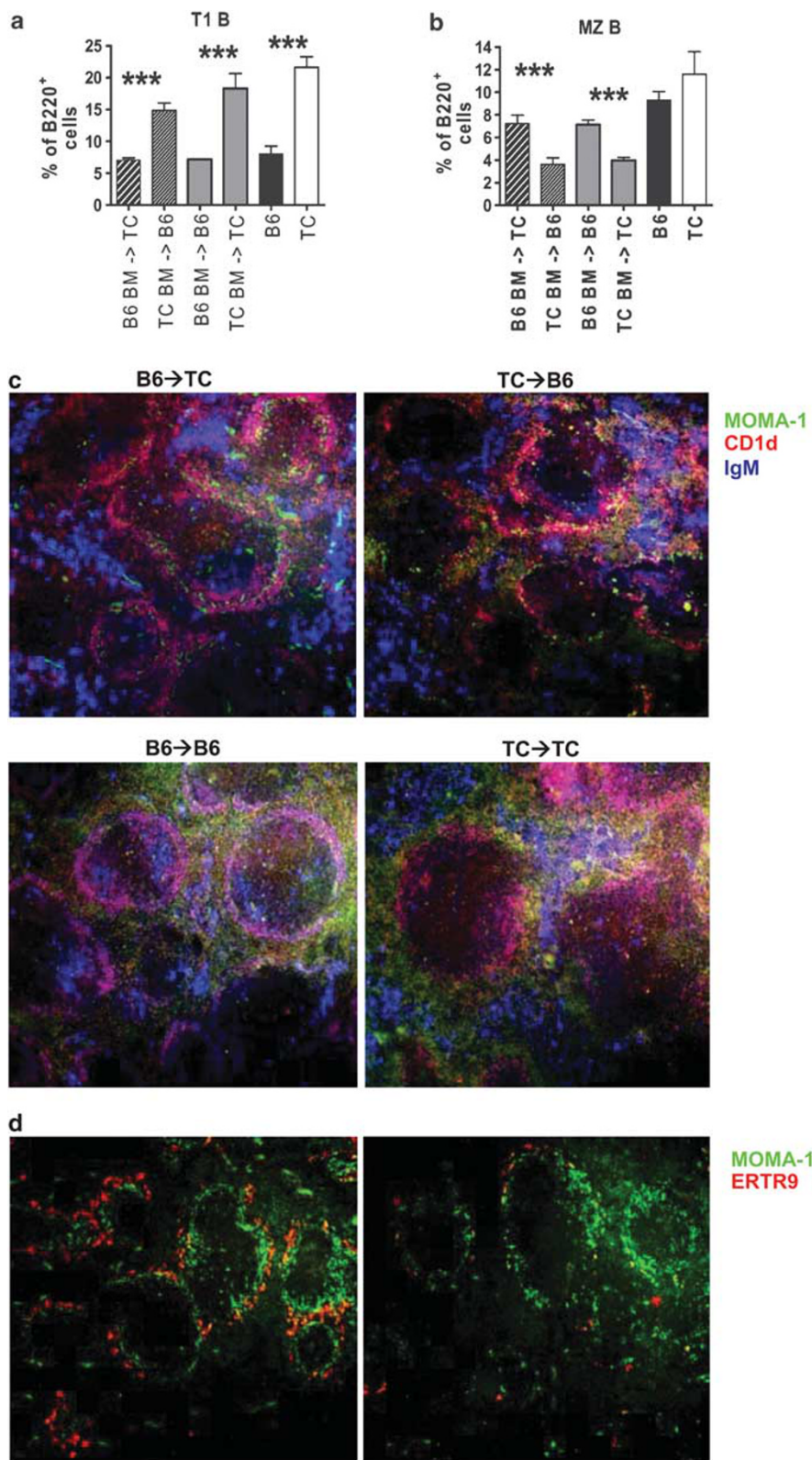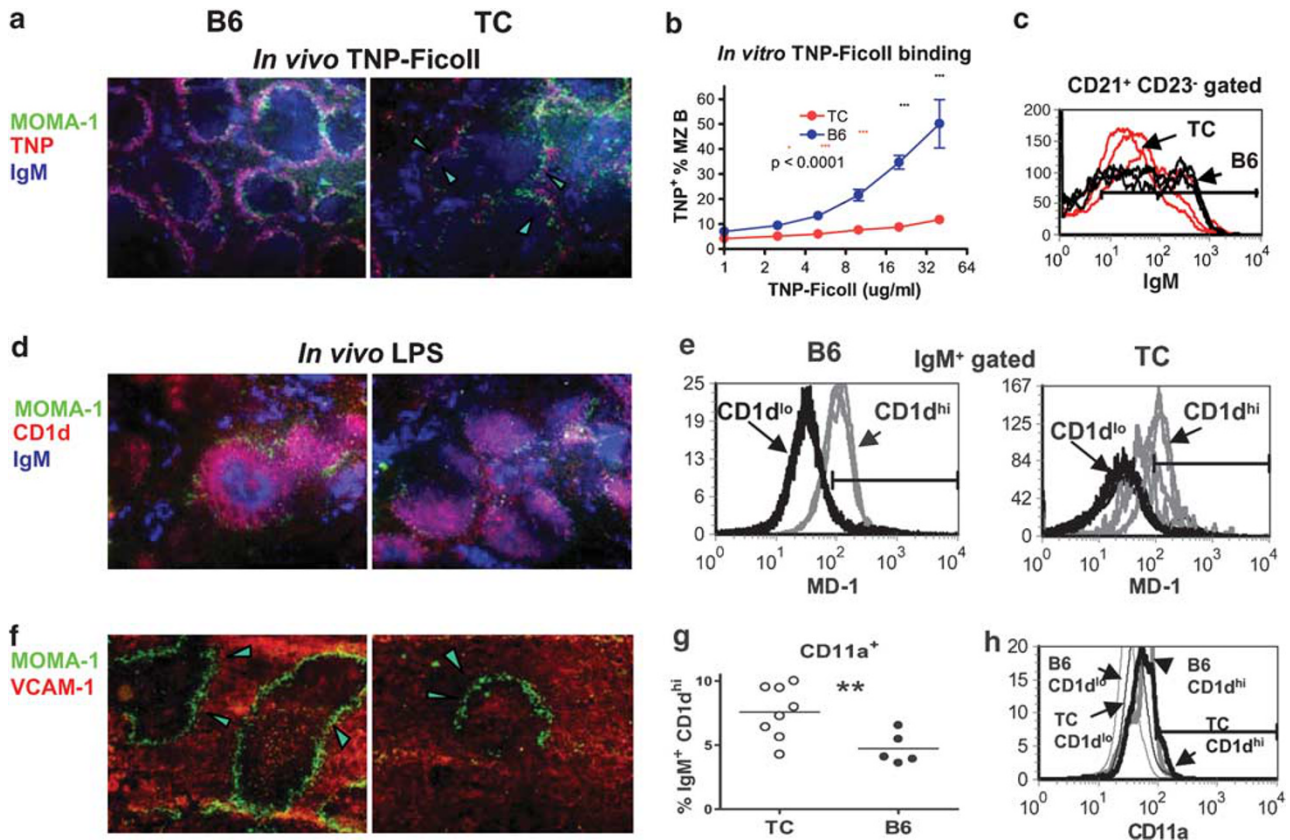
Figure 4 B6.TC MZ B cells show defective functions. (**a**) *In vivo* TNP-Ficoll binding detected 30 min post i.p. injection. (**b**) *In vitro* TNP-Ficoll binding on splenocyte single cell suspensions incubated with graded concentrations of TNP-Ficoll, detected with anti-TNP Ab on IgM$^+$ CD21$^+$ CD23$^-$-gated MZ B cells. The graph shows means and s.e. of four mice per strain. The two regression lines were compared with the comparison of fits. (**c**) Representative IgM expression on B6 (black) and B6.TC (red) CD21$^+$ CD23$^-$ splenocytes. (**d**) Location of B6 (left) and B6.TC (right) IgM$^+$ CD1d$^+$ cells relative to the MOMA-1$^+$ ring 3 h after LPS injection. (**e**) Representative MD-1 expression on IgM$^+$ CD1d$^+$ (three gray histograms) and IgM$^+$ CD1d$^-$ cells (three black histograms) in B6 (left panel) and B6.TC (right panel) mice. (**f**) VCAM-1 expression showing a relative decrease in the B6.TC MZ (right) as compared to B6 (left). (**g**) CD11a expression was significantly increased on IgM$^+$ CD1d$^+$ B cells in B6.TC mice. (**h**) Representative CD11a expression in B6 (gray histograms) and B6.TC (black histograms) IgM$^+$ CD1d$^+$ (thick lines) and IgM$^+$ CD1d$^-$ B cells (thin lines). In each histogram, the position of the marker for positive staining was based on the appropriate isotype control. *$P<0.05$, **$P<0.01$. (**a**, **d**, and **f**) Representative sections of five 7- to 9-month-old mice per strain (magnification $\times 100$).

location in 3 month chimeras, the disorganization of the B6.TC follicular structure results from both BM- and stromal-derived factors.

Interestingly, the paucity of B6.TC MZMs was entirely BM-derived (Figure 3d) and was dissociated from retention of IgM$^+$ CD1d^{hi}/MZ B cells in the MZ area. MZM numbers and distribution in both B6 and B6.TC control syngeneic chimeras were similar to that of the corresponding unmanipulated mice (data not shown). This suggested that contrary to gene-targeted models,[9,10] MZMs and MZ B cells are not dependent on each other for MZ location in the B6.TC model.

B6.TC MZ B Cells are Functionally Defective

To assess B6.TC MZ B-cell function, we analyzed their *in vivo* ability to bind TNP-Ficoll, a TI type 2 (TI-2) antigen used as a model for blood-borne Gram$^+$ bacteria. TNP-Ficoll binding was intense and confined to the B6 MZ, but it was sparser in the B6.TC MZ area and scattered in the follicles (Figure 4a). To control for accessibility of the B6.TC

intrafollicular MZ B cells to blood flow, splenocytes were exposed *in vitro* to graded concentrations of TNP-Ficoll and TNP binding was assessed by flow cytometry. As expected, TNP binding was only found in IgM$^+$ CD21$^+$ CD23$^-$ B cells in both strains (data not shown). Even at the lowest Ficoll concentration ($\leq 5\,\mu g/ml$), significantly fewer B6.TC MZ B cells bound TNP than B6 ($P<0.01$), and the difference between the two dose–responses was highly significant ($P<0.0001$, Figure 4b). Similar results were obtained when the amount of TNP binding per MZ B cell was compared between the two strains (data not shown). Consequently, both the *in vivo* and *in vitro* results concurred in showing an impaired binding of TI-2 antigens by B6.TC MZ B cells regardless of their location. A possible contributing factor to this phenotype was a reduced surface IgM expression on B6.TC MZ B cells (geometric mean fluorescence intensity (MFI): B6: 77.81 ± 14.31, B6.TC: 38.07 ± 6.12, $N = 15$, $P<0.01$), with the striking absence of IgM^{hi} cells in B6.TC MZ B cells (Figure 4c). This reduced B-cell receptor (BCR) expression suggests a higher level of antigen exposure, as

should be expected in autoreactive cells. It should be noted, however, that B6.TC mice produce a robust anti-Ficoll Ab response (data not shown), which indicates that the deficiency in Ficoll binding by B6.TC MZ B cells is compensated by other factors that may include an increased number of B-1a cells.

Multiple Mechanisms Contribute to B6.TC MZ B-Cell Location

We hypothesized that the B6.TC CD1d^hi/MZ B-cell intrafollicular location may result from an aberrant response to LPS. As expected, the entire B6 CD1d^hi/MZ B population migrated inside the follicles and B6.TC MZ B-cell intrafollicular population was denser upon LPS stimulation, suggesting that the extra-follicular B6.TC MZ B cells migrated in response to LPS (compare Figures 2b and 4d). MZ B cells respond rapidly to LPS due to their high expression of the TLR4 complex.[32] As expected, the expression of the MD-1/RP105 component of TLR4 was much greater on B6 IgM^+ CD1d^hi than IgM^+ CD1d^lo non-MZ B cells (Figure 4e). In contrast, MD-1 expression on B6.TC IgM^+ CD1d^hi cells was more variable and tended to be lower than on B6. Consequently, B6.TC IgM^+ CD1d^hi/MZ B-cell intrafollicular location is not due to an increased TLR4 expression.

Normal retention of MZ B cells is achieved through integrins LFA-1 and $\alpha 4/\beta 1$ binding to their ligands ICAM-1 and VCAM-1 expressed on MZ stromal cells. To test if these interactions were deficient in B6.TC mice, we examined MZ ICAM-1 and VCAM-1 expression by immunofluorescence, and the level of CD11a (LFA-1 α chain) and CD29 (integrin $\beta 1$ chain) on MZ B cells by flow cytometry. ICAM-1 expression pattern was similar between B6.TC and B6 MZ region (data not shown), but VCAM-1 expression was less intense in B6.TC than in B6 MZ area (Figure 4f). Unexpectedly, there was a significantly increased CD11a expression on B6.TC IgM^+ CD1d^hi B cells as compared to B6 (Figures 4g and h), but that difference must be too small to favor the retention of these cells in the MZ area. CD29 expression was similar between B6 and B6.TC MZ B cells (data not shown).

CXCR5 directs B cells to migrate toward the follicles where the level of the chemokine CXCL13 is the highest. B6.TC IgM^+ CD1d^hi (Figures 5a and b) and IgM^+ CD21^+ CD1d^hi (Figures 5c and d) B cells expressed significantly higher levels of CXCR5 as compared to B6, and this difference did not exist between the IgM^+ CD1d^lo non-MZ B compartments. This increased CXCR5 expression was concomitant with B6.TC IgM^+ CD1d^hi B cells migrating significantly more in response to CXCL13 (Figure 5e). In addition, B6.TC IgM^+ CD1d^hi B cells showed increased migration to S1P (Figure 5f). Overall, these data suggest that decreased VCAM-1 expression by MZ stromal cells combined with increased migration to CXCL13 and S1P account, at least in part, for the intrafollicular location of B6.TC MZ B cells.
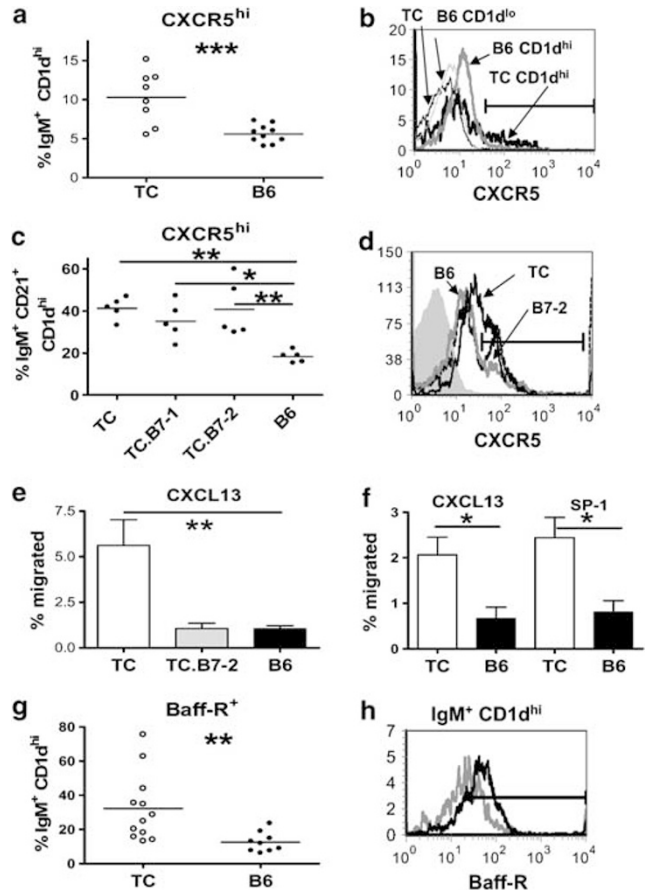
Figure 5 B6.TC MZ B cells showed an increased response to CXCL13 and S1P. (**a**) CXCR5^hi expression on IgM^+ CD1d^hi-gated MZ B cells. (**b**) Representative histograms of CXCR5 expression on IgM^+ CD1d^hi MZ B cells (thick lines) and IgM^+ CD1d^− non-MZ B cells (thin lines) in B6 (gray histograms) and B6.TC (black histograms) mice. (**c**) CXCR5^hi expression on IgM^+ CD21^+ CD1d^hi-gated MZ B cells from B6.TC, B6.TC.B7-1^−/−, B6.TC.B7-2^−/−, and B6 mice. (**d**) Representative histograms of CXCR5 expression on IgM^+ CD21^+ CD1d^hi MZ B cells in B6 (gray) and B6.TC (heavy black) and mice B6.TC.B7-2^−/− (thin black). The filled gray histogram shows the CXCR5 isotype control. (**e**) Percentage of IgM^+ CD1d^+ B cells from B6.TC (white), B6.TC.B7-2^−/− (gray), and B6 (black) mice that migrated to CXCL13. (**f**) Percentage of IgM^+ CD1d^+ B cells from B6.TC (white) and B6 (black) mice that migrated to CXCL13 or S1P. (**c** and **d**) Means and s.e. of four mice per groups. (**g**) BAFF-R expression on IgM^+ CD1d^+-gated MZ B cells with representative histograms for B6.TC (black) and B6 (gray) shown in (**h**). The position of the marker for positive staining was based on the isotype control. *$P < 0.05$, **$P < 0.01$, ***$P < 0.001$. (**a**, **f**, **g**) t-Tests, (**c** and **e**) Dunnett's multiple comparison test with B6 as controls.

BAFF-R expression, which is high on MZ B cells,[33] was significantly higher on B6.TC than on B6 IgM^+ CD1d^hi B cells (Figures 5g and h). This was however not specific to MZ B cells as BAFF-R expression was also significantly higher on total B6.TC B cells as compared to B6 ($P < 0.05$). Increased BAFF-R expression by B6.TC B cells may result from increased BCR signaling,[34] and/or reflect that autoreactive B cells require more BAFF for survival,[35] but it is unlikely to account for the specific MZ B phenotypes in B6.TC mice.

B7-2 Deficiency Alleviates Autoimmune Pathology and Restores IgM⁺ CD1d^hi/MZ B-Cell Retention in the in B6.TC MZ

B7-2 but not B7-1 deficiency abrogated the production of anti-dsDNA (Figure 6a) and anti-chromatin IgG (data not shown) and significantly reduced the production of total IgG (Figure 6b) but not IgM (data not shown) in B6.TC mice. Renal pathology was significantly reduced by both B7-1 and B7-2 deficiency (Figures 6c–f), but this improvement was significantly greater in B6.TC.B7-2$^{-/-}$ mice. CD23 expression on B cells was also increased by both B7-1 and B7-2 deficiency (Figure 6g), but B7-2 deficiency had a more profound effect, as B6.TC.B7-2$^{-/-}$ mice had a normal CD23$^+$ follicular B-cell compartment as detected both by flow cytometry (data not shown) and by immunohistochemistry (Figure 7a). A well-developed MZ B population was also apparent in B6.TC.B7-2$^{-/-}$ but not in B6.TC.B7-1$^{-/-}$ spleens. In fact, more than 50% of the B6.TC.B7-2$^{-/-}$ splenic H&E sections revealed an MZ thickness equivalent to B6, and over 40% of them were hyperplastic. This was significantly different from B6.TC, in which 98% of the spleens showed reduced MZ thickness (Figure 6h). In contrast, only 25% of the B6.TC.B7-1$^{-/-}$ MZs had normal thickness, and none were hyperplastic. Most IgM⁺ CD1d^hi cells were excluded from the follicles in B6.TC.B7-2$^{-/-}$, but not in B6.TC.B7-1$^{-/-}$ mice (Figure 7b). Coincidentally, the response of B6.TC.B7-2$^{-/-}$ MZ B cells to CXCL13 was restored to B6 levels (Figure 5e), although B6.TC.B7-2$^{-/-}$ MZ B cells express high levels of CXCR5 (Figures 5b and c). Finally, normal numbers and location of ETR9⁺ MZMs were also restored by B7-2 but not B7-1deficiency (Figure 7c). These results indicate that increased B7-2 activation is involved in the abnormal B6.TC IgM⁺ CD1d^hi/MZ B phenotypes. B7-2 expression was higher on total B6.TC B cells than in B6 (Morel et al[23]; data not shown), but it was similar between ex vivo B6.TC and B6 IgM⁺ CD21⁺ CD23⁻ or IgM⁺ CD1d⁺ MZ B cells, although high levels of in vitro anti-IgM stimulation induced a significantly higher B7-2 expression on B6.TC MZB cells (Supplementary Figure 2). The other activation markers CD80 and CD69 were also expressed at similar levels between B6.TC and B6 MZ B cells (data not shown).

DISCUSSION

B6.TC mice show an abnormal splenic B-cell development with a striking proportional decrease in CD23$^+$ B cells that is correlated with autoantibody production and T-cell activation. We have previously shown that transitional T1 B cells, which are CD23⁻, accumulate in B6.TC spleens,[19,27] suggesting a defect in the check point that eliminates the large number of autoreactive clones emerging from the BM.[36] We have shown that MZ B cells, the other CD23⁻ B-cell subset apart from plasma cells, represent an increased percentage of splenic B cells in B6.TC mice as compared to B6 (Duan et al and Xu et al[19,27] and this report). An enlargement of the MZ B-cell compartment has been described and implicated in
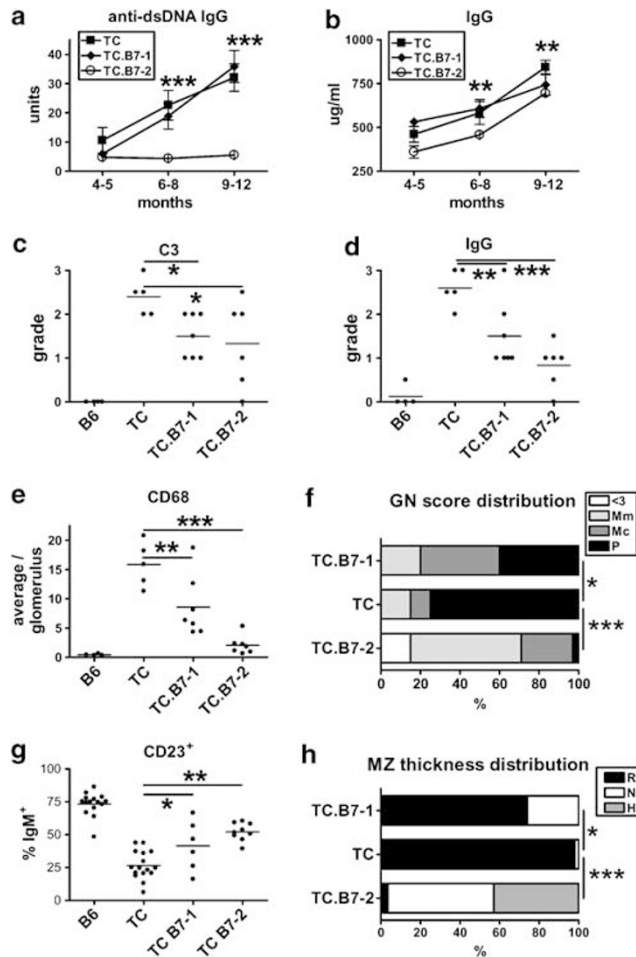
Figure 6 B7-2 but not B7-1 deficiency decreased autoimmune pathology in B6.TC and increased their MZ size. Anti-dsDNA IgG (**a**) and total IgG (**b**) production in female mice according to age in months. Means and s.e. of 20 mice per group, statistical significance of t-tests between B6.TC and B6.TC.B7-2$^{-/-}$ values; **P < 0.01, ***P < 0.0001. Complement C3 (**c**), IgG (**d**) deposits, and CD68$^+$ cellular infiltrates (**c**) in glomeruli quantified on frozen kidney sections. (**f**) Distribution of severe (3–4+) GN, with white sections representing negative to mild GN scores (0–2), and shaded sections indicating the severe scores (3–4) partitioned by type of lesion: light gray for mesangial matrix increase (Mm); dark gray for hypercellularity limited to the mesangium (Mc) and black for proliferative or necrotizing lesions involving the capillary loops (P). Percentages of the various scores were tabulated on 25 B6.TC, 20 B6.TC.B7-1$^{-/-}$ and 33 B6.TC.B7-2$^{-/-}$ mice at killing (either when proteinuric or at 10- to 12-month old). (**g**) CD23 expression on IgM$^+$ B cells from 9- to 12-month-old mice. (**h**) MZ thickness distribution measured on splenic H&E sections relative to B6 (N, normal; R, reduced; H, hyperplastic) from the same mice evaluated for GN in (**f**). (**c–e** and **g**) Statistical significance of Bonferroni's multiple comparison tests between B6.TC and either B6.TC.B7-1$^{-/-}$ or B6.TC.B7-2$^{-/-}$ values. (**f** and **g**) χ^2-Statistics for pair-wise comparisons between B6.TC and either B6.TC.B7-1$^{-/-}$ or B6.TC.B7-2$^{-/-}$. *P < 0.05; **P < 0.01; ***P < 0.0001.

murine models of lupus,[14–17] and type I diabetes.[30] What sets the B6.TC MZ B cells apart is their intrafollicular location. MZ B cells are more potent T-cell activators that respond more rapidly than follicular B cells to TD antigens,[3] and are essential role in transporting antigens to the follicle.[37] MZ B cells also differentiate rapidly into plasma cells in response to either TD
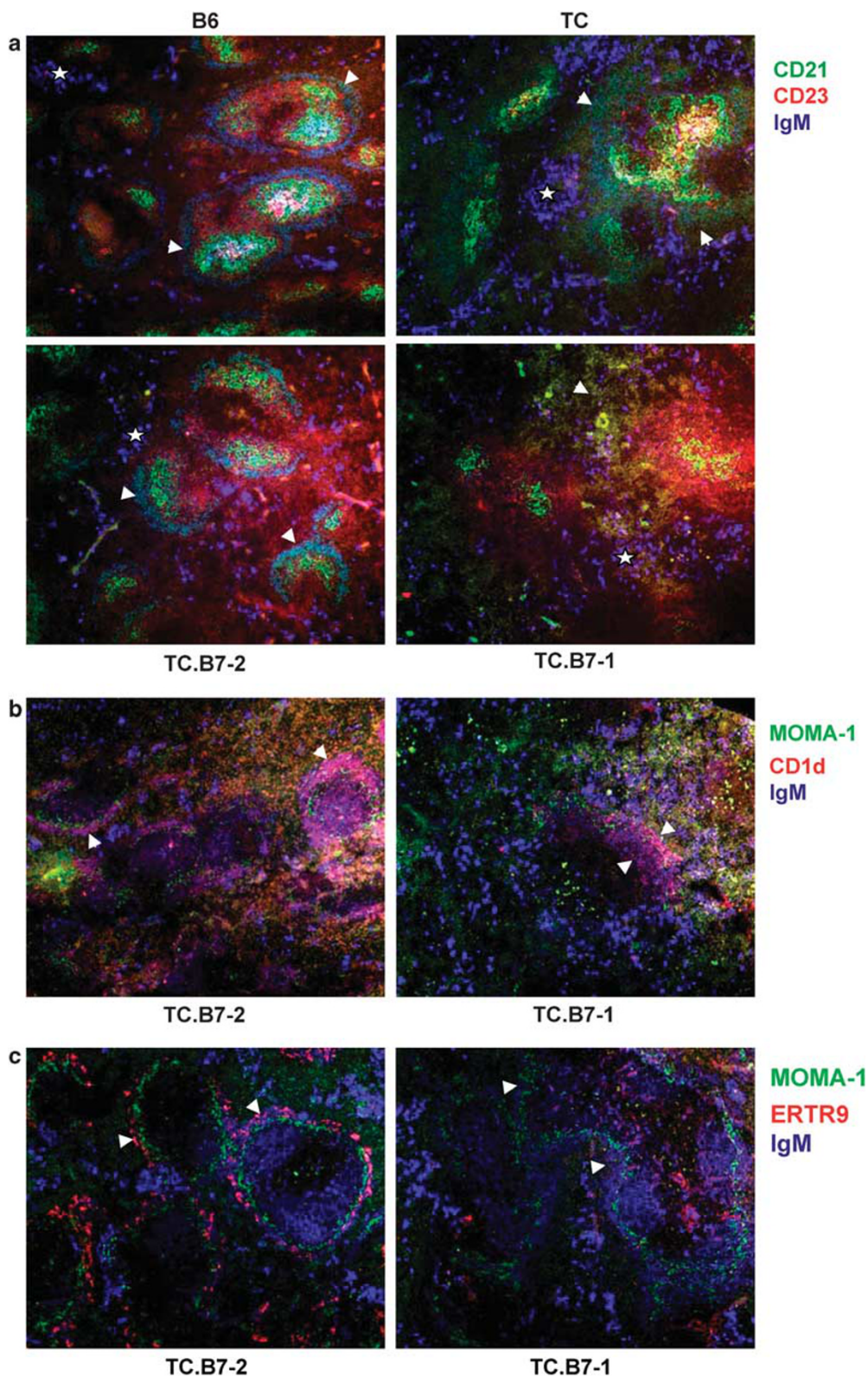
Figure 7 B7-2 but not B7-1 deficiency restored B-cell follicular structure, IgM$^+$ CD1d^{hi} cell location in the marginal zone, and MZM numbers and location in B6.TC mice. (**a**) CD21, CD23, and IgM triple staining revealed that B7-2 deficiency restored MZ (indicated by arrowheads) and follicular B-cell structure, and CD23 expression on B cells. Star symbols indicate plasma cell clusters. (**b**) B-2 deficiency restores IgM$^+$ CD1d$^+$ B cells outside of the MOMA-1$^+$ ring, as indicated by arrowheads. IgM$^+$ CD1d$^+$ cells present in B6.TC.B7-1$^{-/-}$ spleens straddle the MOMA-1$^+$ layer. (**c**) B-2 but not B7-1 deficiency restores ETR9$^+$ MZM numbers and location in the marginal zone, as indicated by arrowheads. Representative sections of at least ten 7- to 9-month-old mice per strain. For **b** and **c** controls, see Figures 2b and c, respectively (magnification × 100).

and TI stimulation.[24,32,38] These observations have led to the hypothesis that sequestration of MZ B cells away from the follicles in an area with very few T cells was a part of the follicular exclusion checkpoint in B-cell tolerance.[16,39] We show here that in the B6.TC lupus model, a large number of IgM$^+$ CD1d^{hi} cells, 80% of which express MZ B-cell surface markers, reside inside the follicles, and that B7-2 deficiency restores follicular exclusion of these IgM$^+$ CD1d^{hi}/MZ B cells. The normalization of the MZ B-cell phenotype in B6.TC.B7-2$^{-/-}$ correlated with nuclear antigen tolerance and significantly reduced renal pathology, suggesting that MZ B-cell follicular exclusion represents an important checkpoint for B-cell tolerance.

The localization and migration of MZ B cells is a balanced outcome controlled by multiple factors.[40] Reciprocal BM transfers between B6 and B6.TC mice showed near normal IgM$^+$ CD1d^{hi}/MZ B-cell location in both directions. The most likely explanation for our results is that both stromal and hematopoietic cells are necessary but not sufficient to determine the B6.TC IgM$^+$ CD1d^{hi}/MZ B-cell location.

Elevated levels of CXCR5 on B6.TC IgM$^+$ CD1d^{hi}/MZ B cells and greater migration of these cells in response to CXCL13 suggests that this chemokine contributes to the MZ B-cell intrafollicular location in B6.TC mice, in agreement with recent data showing that MZ B migration to the follicle was CXCR5-dependent.[37] The fact that B6.TC.B7-2$^{-/-}$ MZ B cells express high CXCR5 levels, but respond poorly to CXCR13 is still consistent with this hypothesis, but the discrepancy between receptor expression and response to the chemokine will have to be addressed in that strain. In normal MZ B cells, CXCR5 response to CXCL13 is abrogated by other factors. LFA-1 and α4β1 integrins expressed by B cells interact with ICAM-1 and VCAM-1, respectively on stromal cells to direct B cells to the white pulp.[41] MZ B cells express higher levels of LFA-1 and α4β1 than follicular B cells, and ablation of integrin binding causes the release of MZ B cells to the peripheral blood.[6] B6.TC IgM$^+$ CD1d^{hi}/MZ B cells express a slightly higher LFA-1 level than B6 that may indicate a higher level of BCR activation.[42] However, immunofluorescence staining suggested a high VCAM-1 expression in B6 MZ but a uniformly lower VCAM-1 expression across B6.TC white pulp. Overall, this is predicted to result in a greater scattering of B6.TC IgM$^+$ CD1d^{hi}/MZ B cells, which were less retained in the MZ. Another factor that abrogates MZ B-cell migration to CXCL13 are the S1P receptors, which are expressed at higher levels on MZ B cells than on follicular B cells, and therefore prevent them from entering the follicles.[7,37] MZ B cells from mice lacking both CXCL13 and S1P receptors did not migrate to the follicles in response to antigen stimulation,[7] suggesting an important balance among integrins, S1P, and CXCL13. Thus in the case of B6.TC IgM$^+$ CD1d^{hi}/MZ B cells, in which S1P level of expression is unknown, high CD11a levels favors their retention but the higher migration to CXCL13 combined with lower VCAM-1 on MZ stromal cells are likely to tip the balance toward follicular migration.

A consistent finding in the B6.TC model is a marked reduction of CD23$^+$ B cells. A recent *in vivo* analysis of CD23 and CD21 expression has suggested a model by which MZ B cells mature directly from T1 (T1a) transitional B cells leaving CD23 transcriptionally inactive in this T1a→MZ B-cell lineage while CD23 is switched on in the T1a→T1b→T2→Follicular pathway.[43] This differentiation model may dominate in B6.TC mice in which IgM$^+$ CD93$^-$ CD21^{hi} CD23$^+$ MZ B precursors are extremely reduced.[19] Therefore B6.TC IgM$^+$ CD1d^{hi}/MZ B cells may be largely derived from T1 transitional B cells that are abnormal either because they have survived too long, have received abnormal T-cell help, and/or display abnormal BCR signaling, all of which are phenotypes that have been described for B cells in this model.[44,45] This aberrant ontogeny may be at the root of the abnormal location and function of B6.TC IgM$^+$ CD1d^{hi}/MZ B cells.

An important clue provided by this study was that B7-2 but not B7-1 deficiency restored normal MZ B-cell location as well as nuclear antigen tolerance and significantly reduced renal pathology in the B6.TC mouse. Only the targeting of both B7-1 and B7-2 with either blocking Abs or genetic engineering was able to offer a significant protection from clinical disease in the MRL/lpr model, with a relatively greater impact of B7-2 deficiency on autoantibody production.[46] The B7-1 and B7-2 molecules bind preferentially to CTLA-4 and CD28, respectively,[47–50] and B7-1 also binds to the negative regulator PDL-1.[51] The exact mechanism by which B7-2 deficiency protects B6.TC mice from autoimmune pathogenesis will require the separate evaluation of the various cell types in which this co-stimulatory molecule is expressed. B7-2 but not B7-1 is upregulated on MZ B cells after BCR engagement,[4] but B7-2 expression on IgM$^+$ CD1d^{hi}/MZ B cells was equivalent between B6.TC and B6. Moreover, we did not observe the BCR-dependent expansion of a B7-2^{hi} of B6.TC MZ B population as described in NZB mice.[52] These results indicate that that B7-2 does not affect the B6.TC MZ B-cell phenotypes directly through its overexpression. B7-2 activation induces B-cell proliferation and immunoglobulin secretion, at least in part through increasing the expression of Bcl-w and Bcl-xL and decreasing capase-8 expression.[53] B7-2 signaling also increases the NF-κB, PI3K, PLCγ2, and PKCαβ pathways in B cells,[54,55] each of which is highly activated in B cells in our model,[45] suggesting that at least one of these pathways is responsible for the B6.TC IgM$^+$ CD1d^{hi}/MZ B intrafollicular location. We hypothesize that the absence of B7-2 signaling resets a pathway that is aberrant in B6.TC MZ B cells due to yet unknown primary defects. None of the individual *Sle* loci is sufficient to induce MZ B-cell intrafollicular location (L Morel, unpublished), which indicates a complex mechanism requiring interactions of multiple genetic defects.

1. Kraal G, Mebius R. New insights into the cell biology of the marginal zone of the spleen. Int Rev Cytol 2006;250:175–215.

2. Martin F, Oliver AM, Kearney JF. Marginal zone and B1B cells unite in the early response against T-independent blood-borne particulate antigens. Immunity 2001;14:617–629.

3. Attanavanich K, Kearney JF. Marginal zone, but not follicular B cells, are potent activators of naive CD4 T cells. J Immunol 2004;172:803–811.

4. Oliver AM, Martin F, Kearney JF. IgM(high)CD21(high) lymphocytes enriched in the splenic marginal zone generate effector cells more rapidly than the bulk of follicular B cells. J Immunol 1999;162:7198–7207.

5. Ansel KM, Ngo VN, Hyman PL, et al. A chemokine-driven positive feedback loop organizes lymphoid follicles. Nature 2000;406:309–314.

6. Lu TT, Cyster JG. Integrin-mediated long-term B cell retention in the splenic marginal zone. Science 2002;297:409–412.

7. Cinamon G, Matloubian M, Lesneski MJ, et al. Sphingosine 1-phosphate receptor 1 promotes B cell localization in the splenic marginal zone. Nat Immunol 2004;5:713–720.

8. Vora KA, Nichols E, Porter G, et al. Sphingosine 1-phosphate receptor agonist FTY720-phosphate causes marginal zone B cell displacement. J Leukoc Biol 2005;78:471–480.

9. Karlsson MCI, Guinamard R, Bolland S, et al. Macrophages control the retention and trafficking of B lymphocytes in the splenic marginal zone. J Exp Med 2003;198:333–340.

10. Nolte MA, Arens R, Kraus M, et al. B cells are crucial for both development and maintenance of the splenic marginal zone. J Immunol 2004;172:3620–3627.

11. Lopes-Carvalho T, Kearney JF. Development and selection of marginal zone B cells. Immunol Rev 2004;197:192–205.

12. Dammers PM, Visser A, Popa ER, et al. Most marginal zone B cells in rat express germline encoded Ig V_H genes and are ligand selected. J Immunol 2000;165:6156–6169.

13. Dunn-Walters DK, Isaacson PG, Spencer J. Analysis of mutations in immunoglobulin heavy chain variable region genes of microdissected marginal zone (MGZ) B cells suggests that the MGZ of human spleen is a reservoir of memory B cells. J Exp Med 1995;182:559–566.

14. Wither JE, Roy V, Brennan LA. Activated B cells express increased levels of costimulatory molecules in young autoimmune NZB and (NZB × NZW)F-1 mice. Clin Immunol 2000;94:51–63.

15. Grimaldi CM, Michael DJ, Diamond B. Cutting edge: expansion and activation of a population of autoreactive marginal zone B cells in a model of estrogen-induced lupus. J Immunol 2001;167:1886–1890.

16. Li YJ, Li H, Weigert M. Autoreactive B cells in the marginal zone that express dual receptors. J Exp Exp 2002;195:181–188.

17. Wither JE, Loh C, Lajoie G, et al. Colocalization of expansion of the splenic marginal zone population with abnormal B cell activation and autoantibody production in B6 mice with an introgressed New Zealand Black chromosome 13 interval. J Immunol 2005;175:4309–4319.

18. Mackay F, Woodcock SA, Lawton P, et al. Mice transgenic for BAFF develop lymphocytic disorders along with autoimmune manifestations. J Exp Med 1999;190:1697–1710.

19. Duan B, Croker BP, Morel L. Lupus resistance is associated with marginal zone abnormalities in an NZM murine model. Lab Invest 2007;87:14–28.

20. Hippen KL, Tze LE, Behrens TW. CD5 maintains tolerance in anergic B cells. J Exp Med 2000;191:883–889.

21. Liu Y, Li L, Kumar KR, et al. Lupus susceptibility genes may breach tolerance to DNA by impairing receptor editing of nuclear antigen-reactive B cells. J Immunol 2007;179:1340–1352.

22. Li Y, Li H, Ni D, et al. Anti-DNA B cells in MRL/lpr mice show altered differentiation and editing pattern. J Exp Med 2002;196:1543–1552.

23. Morel L, Croker BP, Blenman KR, et al. Genetic reconstitution of systemic lupus erythematosus immunopathology with polycongenic murine strains. Proc Natl Acad Sci USA 2000;97:6670–6675.

24. Oliver AM, Martin F, Gartland GL, et al. Marginal zone B cells exhibit unique activation, proliferative and immunoglobulin secretory responses. Eur J Immunol 1997;27:2366–2374.

25. Freeman GJ, Borriello F, Hodes RJ, et al. Uncovering of functional alternative Ctla-4 counter-receptor in B7-deficient mice. Science 1993;262:907–909.

26. Sobel ES, Mohan C, Morel L, et al. Genetic dissection of SLE pathogenesis: adoptive transfer of Sle1 mediates the loss of tolerance by bone marrow-derived B cells. J Immunol 1999;162:2415–2421.

27. Xu Z, Duan B, Croker BP, et al. STAT4 deficiency reduces autoantibody production and glomerulonephritis in a mouse model of lupus. Clin Immunol 2006;120:189–198.

28. Erickson LD, Lin LL, Duan B, et al. A genetic lesion that arrests plasma cell homing to the bone marrow. Proc Natl Acad Sci USA 2003;100:12905–12910.

29. Makowska A, Faizunnessa NN, Anderson P, et al. CD1high B cells: a population of mixed origin. Eur J Immunol 1999;29:3285–3294.

30. Rolf J, Motta V, Duarte N, et al. The enlarged population of marginal zone/CD1dhigh B lymphocytes in nonobese diabetic mice maps to diabetes susceptibility region Idd11. J Immunol 2005;174:4821–4827.

31. Mohan C, Yu Y, Morel L, et al. Genetic dissection of Sle pathogenesis: Sle3 on murine chromosome 7 impacts T cell activation, differentiation, and cell death. J Immunol 1999;162:6492–6502.

32. Gunn KE, Brewer JW. Evidence that marginal zone B cells possess an enhanced secretory apparatus and exhibit superior secretory activity. J Immunol 2006;177:3791–3798.

33. Ng LG, Sutherland AP, Newton R, et al. B cell-activating factor belonging to the TNF family (BAFF)-R is the principal BAFF receptor facilitating BAFF costimulation of circulating T and B cells. J Immunol 2004;173:807–817.

34. Smith SH, Cancro MP. Cutting Edge: B cell receptor signals regulate BLyS receptor levels in mature B cells and their immediate progenitors. J Immunol 2003;170:5820–5823.

35. Lesley R, Xu Y, Kalled SL, et al. Reduced competitiveness of autoantigen-engaged B cells due to increased dependence on BAFF. Immunity 2004;20:441–453.

36. Srivastava B, Lindsley RC, Nikbakht N, et al. Models for peripheral B cell development and homeostasis. Semin Immunol 2005;17:175–182.

37. Cinamon G, Zachariah MA, Lam OM, et al. Follicular shuttling of marginal zone B cells facilitates antigen transport. Nat Immunol 2008;9:54–62.

38. Mandik-Nayak L, Racz J, Sleckman BP, et al. Autoreactive marginal zone B cells are spontaneously activated but lymph node B cells require T cell help. J Exp Med 2006;203:1985–1998.

39. Chen X, Martin F, Forbush KA, et al. Evidence for selection of a population of multi-reactive B cells into the splenic marginal zone. Int Immunol 1997;9:27–41.

40. Cyster JG. Chemokines, sphingosine-1-phosphate, and cell migration in secondary lymphoid organs. Annu Rev Immunol 2005;23:127–159.

41. Lo CG, Lu TT, Cyster JG. Integrin-dependence of lymphocyte entry into the splenic white pulp. J Exp Med 2003;197:353–361.

42. Dang LH, Rock KL. Stimulation of B lymphocytes through surface Ig receptors induces LFA-1 and ICAM-1-dependent adhesion. J Immunol 1991;146:3273–3279.

43. Debnath I, Roundy KM, Weis JJ, et al. Defining in vivo transcription factor complexes of the murine CD21 and CD23 genes. J Immunol 2007;178:7139–7150.

44. Mohan C, Morel L, Yang P, et al. Genetic dissection of systemic lupus erythematosus pathogenesis: Sle2 on murine chromosome 4 leads to B cell hyperactivity. J Immunol 1997;159:454–465.

45. Wu T, Qin X, Kurepa Z, et al. Shared signaling networks active in B cells isolated from genetically distinct mouse models of lupus. J Clin Invest 2007;117:2186–2196.

46. Liang B, Kashgarian MJ, Sharpe AH, et al. Autoantibody responses and pathology regulated by B7-1 and B7-2 costimulation in MRL/lpr lupus. J Immunol 2000;165:3436–3443.

47. Collins AV, Brodie DW, Gilbert RJC, et al. The interaction properties of costimulatory molecules revisited. Immunity 2002;17:201–210.

48. Jansson A, Barnes E, Klenerman P, et al. A theoretical framework for quantitative analysis of the molecular basis of costimulation. J Immunol 2005;175:1575–1585.

49. Pentcheva-Hoang T, Egen JG, Wojnoonski K, et al. B7-1 and B7-2 selectively recruit CTLA-4 and CD28 to the immunological synapse. Immunity 2004;21:401–413.

50. Zheng Y, Manzotti CN, Liu M, et al. CD86 and CD80 differentially modulate the suppressive function of human regulatory T cells. J Immunol 2004;172:2778–2784.

51. Butte MJ, Keir ME, Phamduy TB, et al. Programmed death-1 ligand 1 interacts specifically with the B7-1 costimulatory molecule to inhibit T cell responses. Immunity 2007;27:111–122.

52. Roy V, Bonventi G, Cai Y, et al. Immune mechanisms leading to abnormal B cell selection and activation in New Zealand Black mice. Eur J Immunol 2007;37:2645–2656.

53. Suvas S, Singh V, Sahdev S, et al. Distinct role of CD80 and CD86 in the regulation of the activation of B cell and B cell lymphoma. J Biol Chem 2002;277:7766–7775.

54. Podojil JR, Kin NW, Sanders VM. CD86 and β2-adrenergic receptor signaling pathways, respectively, increase Oct-2 and OCA-B expression and binding to the 3′-IgH enhancer in B cells. J Biol Chem 2004;279:23394–23404.

55. Kin NW, Sanders VM. CD86 stimulation on a B cell activates the phosphatidylinositol 3-kinase/Akt and phospholipase Cγ2/protein kinase C$\alpha\beta$ signaling pathways. J Immunol 2006;176: 6727–6735.